Synthesis, crystal structure, infrared spectrum and thermal behaviour of α-$BaHPO_4$

Henning A. Höppe [a,*], Michael Daub [a], Oliver Oeckler [b]

[a] Institut für Anorganische und Analytische Chemie, Albert-Ludwigs-Universität, Albertstraße 21, D-79104 Freiburg, Germany
[b] Department Chemie, Ludwig-Maximilians-Universität, Butenandtstr. 5-13 (Haus D), D-81377 München, Germany

1. Introduction

Although phosphates are amongst the most thoroughly investigated compounds [1] there is still a lack of knowledge about the structure of many crystalline phosphates. Among these, alkaline earth phosphates, for example, attract interest in materials science, e.g. due to the possibility of doping them with divalent or trivalent rare earth ions to produce efficient fluorescent materials [2–4]. So far, the literature reports about a single polymorph of $BaHPO_4$ [5], which we assume to be a high-temperature polymorph of the barium hydrogen phosphate described in this contribution. Therefore we assign β-$BaHPO_4$ to the older one and suggest to call our low-temperature polymorph α-$BaHPO_4$. Recently an infrared spectrum of α- or β-$BaHPO_4$ was published [6] – the authors just mention that they grew crystals and did not perform any diffraction experiments. Furthermore, the authors made first attempts to clarify the phonon spectrum of α- or β-$BaHPO_4$ [7].

In this contribution the solution of the crystal structure of the possible precursor compound for condensed barium phosphates α-$BaHPO_4$ will be presented and compared with its high-temperature polymorph. Additionally, the infrared spectrum is reported and compared with that published recently [6].

2. Experimental

2.1. Synthesis

The synthesis of α-$BaHPO_4$ was performed in a Petri dish according to eq. (1).

$$4Ba(OH)_2 + P_4O_{10} \rightarrow 4\alpha - BaHPO_4 + 2H_2O \qquad (1)$$

51.4 mg (0.300 mmol) barium hydroxide $Ba(OH)_2$ (Merck, pure) were dissolved in a Petri dish with 10 ml water. 21.3 mg (0.150 mmol) phosphorus pentoxide P_2O_5 (Roth, 98.5%) were added to the solution. The covered Petri dish was put into a compartment drier at 373 K until the water was evaporated (2 d). The reaction yielded single-phase α-$BaHPO_4$ as a crystalline, colourless and non-hygroscopic powder.

2.2. Vibrational spectroscopy

An FTIR spectrum was obtained at room temperature by using a Bruker IFS 66v/S spectrometer. The samples were thoroughly mixed with dried KBr (approx. 2 mg sample, 300 mg KBr).

2.3. Thermal analysis

Thermogravimetric (TG) and differential thermal analysis (DTA) data were obtained between room temperature and 650 °C by

---

* Corresponding author. Tel.: +49 761 203 6106; fax: +49 761 203 6012.
E-mail address: henning.hoeppe@ac.uni-freiburg.de (H.A. Höppe).

Table 1

Crystallographic data of α-$BaHPO_4$ (estimated standard deviations in parentheses).

Crystal data	
$BaHPO_4$	$F(000) = 1664$
$M = 233.32$ g/mol	$\rho_{x\text{-ray}} = 4.196$ g/cm
Orthorhombic	Mo-K_α radiation
Space group *Aem*2 (no. 39)	$\lambda = 0.71073$ Å
$a = 4.5996(9)$ Å	$\mu = 11.04$ mm^{-1}
$b = 22.809(5)$ Å	$T = 293(2)$ K
$c = 14.081(3)$ Å	Crystal shape: plate
$V = 1477.3(5)$ Å^3	$0.01 \times 0.03 \times 0.04$ mm^3
$Z = 16$	Colourless
Data collection	
Bruker AXS CCD APEX II	
Absorption correction: multi-scan	$h = -6 \rightarrow 6$
$T_{\min} = 0.3570$; $T_{\max} = 0.5546$	$k = -26 \rightarrow 32$
$R_\sigma = 0.0568$	$l = -19 \rightarrow 16$
$2\theta_{\max} = 60.0°$	1995 independent reflections
	1473 observed reflections ($F_o^2 \geq 2\sigma(F_o^2)$)
Refinement	
Refinement on F^2	Program used to refine structure: SHELXL-97 [8]
$R1 = 0.069$ (all)/0.042 (obs)	$w^{-1} = \sigma^2 F_o^2 + (xP)^2 + yP$; $P = (F_o^2 + 2F_c^2)/3$
$wR2 = 0.077$ (all)/0.069 (obs)	Weighting scheme (x/y) 0.0251/0
GooF = 1.054	Twin fraction: 0.40(10)
Extinction coefficient: 0.00004(3)	Twin type: inversion
	Min. residual electron density: −1.93 e/Å^3
102 parameters	Max. residual electron density: 1.73 e/Å^3

Table 3

Selected interatomic distances/pm and angles/° for α-$BaHPO_4$ (estimated standard deviations in parentheses).

Ba1–O	275.5(14)–288.9(11)	9 distances
Ba2–O	273.4(8)–301.5(4)	10 distances
Ba3–O	281.1(9)–326.5(11)	8 + 2 distances
Ba–Ba	454.5(1)–472.7(2)	
P–O	150.6(6)–153.5(6)	∅ = 152.0
P–OH	154.8(8)–158.5(7)	∅ = 156.2
O–P–O	107.2(10)–114.7(7)	∅ = 111.0
O–P–OH	100.9(7)–111.9(7)	∅ = 108.4

using a Netzsch Simultan-Thermoanalyzer STA 429. The samples of approx. 50 mg were heated in alumina crucibles against an alumina reference under air flow with a heating rate of 10°/min.

3. Crystal structure and crystallographic classification

3.1. Crystal structure determination

A suitable single crystal of α-$BaHPO_4$ was enclosed in a glass capillary. X-ray diffraction data were collected on a Bruker AXS CCD diffractometer fitted with an APEX-II detector and corrected for absorption by applying a multi-scan correction. The diffraction pattern was indexed on the basis of an *A*-centred orthorhombic unit cell. The crystal structure of α-$BaHPO_4$ was solved by direct methods using SHELXTL [8] in space group *Aem*2 (no. 39) and refined as an inversion twin with anisotropic displacement parameters for all atoms.

The relevant crystallographic data and further details of the X-ray data collection are summarised in Table 1. Table 2 shows the positional and displacement parameters for all atoms. In Table 3 selected interatomic distances and angles are listed.

A sample of α-$BaHPO_4$ was enclosed in a glass capillary with 0.2 mm diameter and investigated at room temperature in Debye–Scherrer geometry on a STOE Stadi P powder diffractometer with Ge(111)-monochromatized Mo-K_α radiation (linear PSD detector, step width 0.5°, acquisition time: 600 s/step). The powder diffraction pattern presented in Fig. 1 shows some amorphous contributions. All reflections have been indexed and their observed intensities are in very good agreement with the calculated diffraction pattern based on the single crystal data.

3.2. Crystal structure

The new structure type of α-$BaHPO_4$ comprises a distorted body-centred arrangement of barium atoms. The quasi-octahedral voids of the resulting structure are occupied by the hydrogen phosphate ions (Fig. 2). The hydrogen atoms could be localised by difference Fourier syntheses and P–O bond length considerations combined with calculations based on the MAPLE concept (MAPLE = Madelung Part of Lattice Energy) [9–11]. Details of the MAPLE calculations can be found as Supplementary material. To maintain reasonable distances to the oxygen atoms the O–H distances were fixed to 99.0(1) pm.

The bond lengths P–O ranging from 150.6(6) to 153.5(6) pm (average 152 pm) are in average shorter than the bond lengths

Table 2

Atomic coordinates, their respective isotropic and anisotropic displacement parameters/Å^2 for α-$BaHPO_4$ (estimated standard deviations in parentheses); the Wyckoff positions are indicated.

Atom	Wyckoff	x	y	z	U_{11}	U_{22}	U_{33}	U_{23}	U_{13}	U_{12}	U_{eq}/U_{iso}
Ba1	*4c*	0.3933(2)	$^3/_4$	0.40844(9)	0.0140(5)	0.0117(7)	0.0133(8)	0.000	−0.0002(6)	0.000	0.0130(3)
Ba2	*8d*	−0.0716(2)	0.62621(4)	0.20370(2)	0.0217(4)	0.0152(6)	0.0150(7)	−0.0010(3)	−0.0011(5)	−0.0003(3)	0.0173(3)
Ba3	*4b*	½	½	0.41063(12)	0.0564(9)	0.0187(7)	0.0170(8)	0.000	0.000	−0.0109(6)	0.0307(4)
P1	*4b*	½	½	0.1647(7)	0.016(2)	0.011(3)	0.029(4)	0.000	0.000	0.001(2)	0.0185(16)
O11	*8d*	−0.5888(17)	0.5523(4)	0.2285(9)	0.019(3)	0.016(4)	0.024(5)	−0.003(2)	−0.001(3)	0.000(3)	0.0197(19)
H11[a]	*8d*	−0.750(4)	0.558(5)	0.2741(8)							0.03
O12	*8d*	−0.7511(19)	0.4805(5)	0.1003(7)	0.019(3)	0.016(4)	0.024(5)	−0.003(2)	−0.001(3)	0.000(3)	0.0197(19)
P2	*4c*	0.4860(13)	$^3/_4$	0.1695(7)	0.014(2)	0.012(4)	0.028(5)	0.000	0.002(2)	0.000	0.0182(18)
O21	*8d*	0.4045(16)	0.6964(4)	0.2277(8)	0.014(4)	0.010(5)	0.021(7)	0.008(3)	0.002(3)	0.005(3)	0.015(3)
O22	*4c*	0.8030(17)	$^3/_4$	0.1407(8)	0.014(4)	0.025(5)	0.011(5)	0.000	0.002(3)	0.000	0.0167(19)
O23	*4c*	0.299(3)	$^3/_4$	0.0764(8)	0.014(4)	0.025(5)	0.011(5)	0.000	0.002(3)	0.000	0.0167(19)
H23	*4c*	0.084(4)	$^3/_4$	0.077(15)							0.03
P3	*8d*	−0.0231(11)	0.62597(13)	0.4455(5)	0.009(2)	0.012(3)	0.005(3)	0.0011(11)	0.0002(15)	−0.0001(17)	0.0087(12)
O31	*8d*	0.003(2)	0.5703(4)	0.3875(7)	0.041(3)	0.018(4)	0.009(5)	0.000(3)	0.005(3)	0.014(3)	0.023(2)
O32	*8d*	−0.120(2)	0.6781(4)	0.3882(9)	0.041(3)	0.018(4)	0.009(5)	0.000(3)	0.005(3)	0.014(3)	0.023(2)
O33	*8d*	0.2481(17)	0.6422(5)	0.5014(7)	0.027(4)	0.036(4)	0.019(4)	0.017(3)	0.002(3)	0.002(3)	0.0273(19)
O34	*8d*	−0.243(2)	0.6116(5)	0.5291(8)	0.027(4)	0.036(4)	0.019(4)	0.017(3)	0.002(3)	0.002(3)	0.0273(19)
H34	*8d*	−0.442(11)	0.625(5)	0.513(10)							0.03

[a] H11: due to chemical reasons the fractional occupational factor was fixed to 0.5.

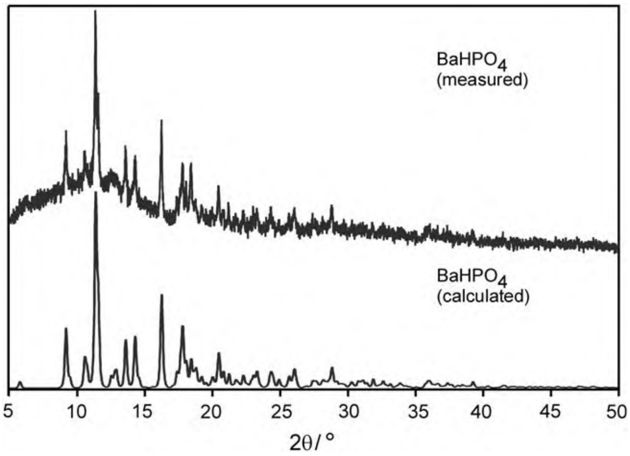

Fig. 1. Observed (top) and calculated (bottom) X-ray powder diffraction pattern (Mo-K$_\alpha$ radiation) of α-BaHPO$_4$.

P–OH (154.8(8)–158.5(7) pm, average 156 pm). They agree well with typical bond lengths in condensed phosphates [1,12,13]. The O–P–O angles vary between 100.9(7)° and 114.7(7)° which also corresponds well with previous structure reports on phosphates.

The deviation from ideal symmetry was calculated applying the method of all ligands enclosing spheres on experimental data. In this method not only distance variations inside a polyhedron but also angle deviations caused by larger distortions are considered. In the first step the optimum centroid of the four surrounding oxygen atoms, i.e. the phosphorus atom, is determined by a least-squares refinement [14] and gives a medium centroid–ligand distance r_{centr}. Subsequently, the volume of an ideal tetrahedron given by eq. (2)

$$\frac{8r_{\mathrm{centr}}^3}{9\sqrt{3}} \tag{2}$$

is calculated using r_{centr}. Finally this volume is compared with the volume of the experimentally obtained body built up by four vertices [15]. This volume can be calculated using eq. (3)

$$\frac{S \cdot h}{3} \tag{3}$$

where S is the base area built from three vertices and h is the height of the body obtained by the distance of the fourth vertex from the base. The three crystallographically different PO$_4$ tetrahedra in α-BaHPO$_4$ feature the values 0.14% (P1), 0.13% (P2) and 0.64% (P3). These values are typical for phosphate tetrahedra found in the recent literature and confirm the consistency of our structure model. In general, the deviations in condensed phosphates are larger compared with those of non-condensed orthophosphates due to the different bonding situations of terminal and bridging oxygen atoms.

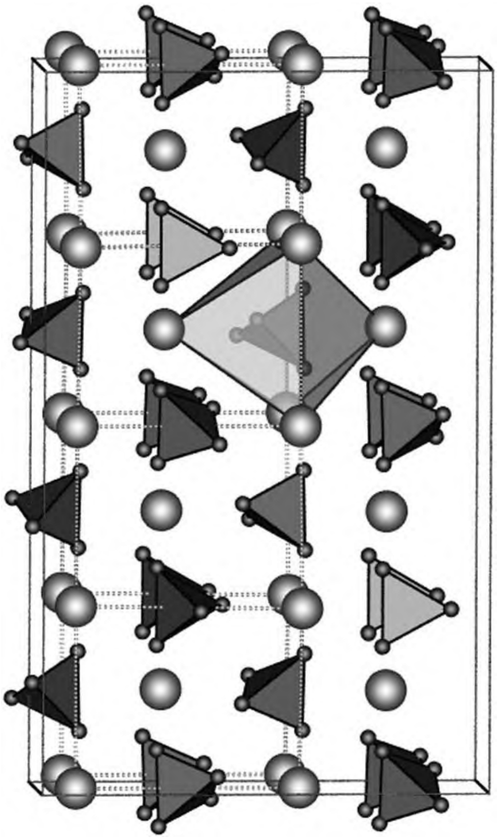

Fig. 2. Overview about the unit cell of α-BaHPO$_4$, the phosphate tetrahedra are drawn as closed polyhedra; a quasi-octahedral void is shown as translucent polyhedron filled with a phosphate tetrahedron; the dotted lines show virtual unit cells of a body-centred packing of the barium atoms.

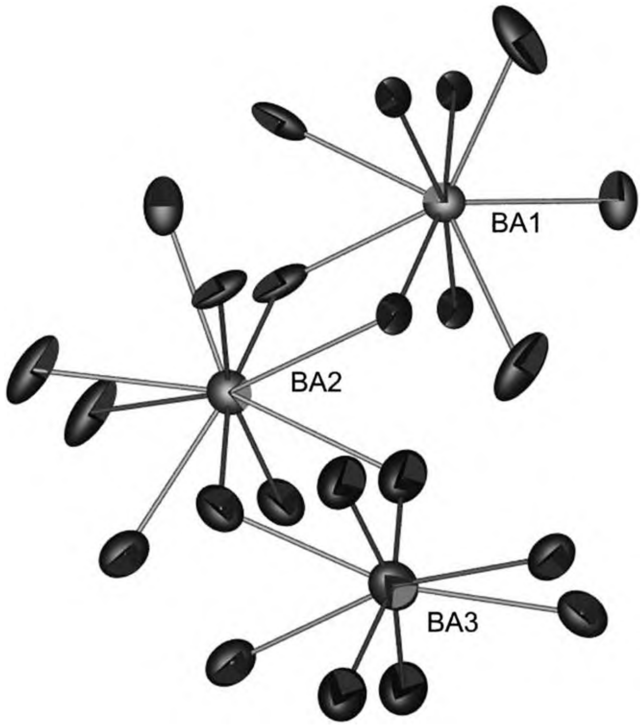

Fig. 3. Representation of the coordination environment of the barium atoms in α-BaHPO$_4$ (Ba: grey, O: dark grey) viewed approx. along [100], the displacement ellipsoids are drawn on a probability level of 95%.

All three crystallographically independent Ba^{2+} ions are coordinated by the oxygen atoms of the hydrogen phosphate anion, the distances Ba–O vary between 273.4(9) and 326.5(11) pm with an average value of 289 pm in good agreement with the sum of ionic radii of 280 pm [16]. Ba(1) is nine-fold, Ba(2) and Ba(3) are ten-fold coordinated (Fig. 3).

Fig. 4 shows the hydrogen bonds found in α-BaHPO$_4$. According to hydrogen bond schemes [17,18] the strength of these can be classified as moderate. An overview of the bonds determined in α-BaHPO$_4$ is given in Table 4.

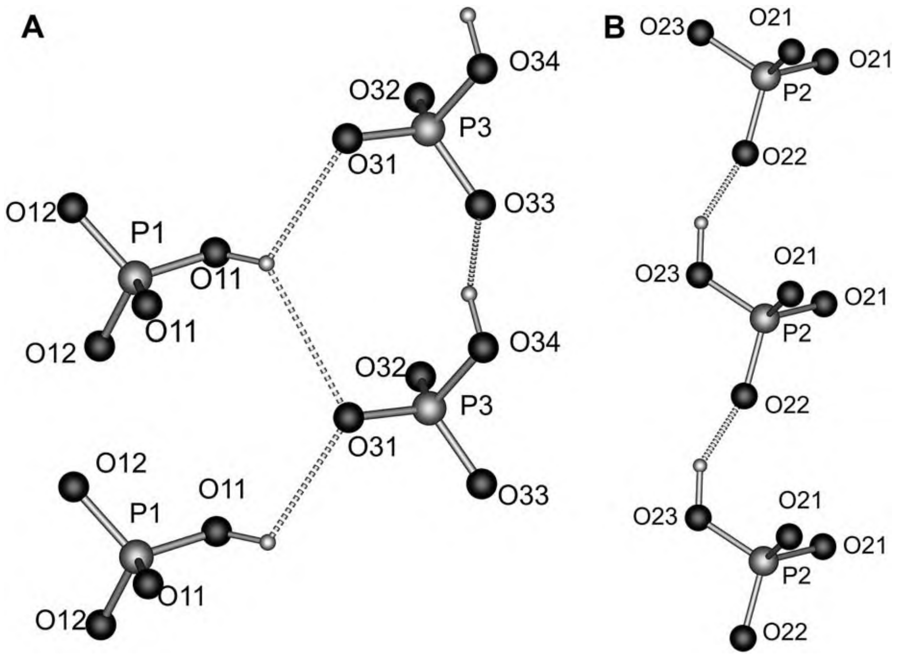

Fig. 4. Visualisation of the hydrogen bonds in α-$BaHPO_4$; the bonds between H and the respective acceptors are dotted.

Further details of the crystal structure investigations may be obtained from the Fachinformationszentrum Karlsruhe, Abt. PROKA, D-76344 Eggenstein-Leopoldshafen, Germany (e-mail: crysdata@fiz-karlsruhe.de) on quoting the depository number CSD-420261, the name of the authors and citation of this publication.

3.3. *Comparison with β-$BaHPO_4$*

The most evident difference between α-$BaHPO_4$ (space group *Aem*2) and β-$BaHPO_4$ (space group *Pbnm*) [5] is the different arrangement of the barium atoms in the unit cell. While in α-$BaHPO_4$ the barium atoms form a distorted body-centred arrangement with edge lengths of the virtual body-centred unit cell of 7.0 Å and 5.7 Å, in β-$BaHPO_4$ a similar arrangement with a larger difference of these edge lengths of 7.2 Å and 4.6 Å is found. Therefore the arrangement of the barium atoms in β-$BaHPO_4$ may be better called sheet-like perpendicular *b* (Fig. 5). In both compounds the phosphate tetrahedra are located in quasi-octahedral voids. The hydrogen bond structure found between the P2 centred tetrahedra in α-$BaHPO_4$ (Fig. 4) resembles that of the P1 centred ones in β-$BaHPO_4$ [5] and the hydrogen bonds between the P3 centred tetrahedra in α-$BaHPO_4$ can be compared with those between the P2 centred ones in β-$BaHPO_4$. Thus both structure types exhibit hydrogen bonding schemes running along the short *a* axis. In the α-polymorph there are additional hydrogen bonds between P1 and P3 centred tetrahedra which are not present in the β-polymorph.

According to the Ostwald–Volmer rule the low-temperature polymorph should have a higher density than the high-temperature polymorph. This is clearly fulfilled in this case since the density ρ_{XRD} of β-$BaHPO_4$ is 4.128 g/cm^3 compared with 4.196 g/cm^3 for α-$BaHPO_4$.

Table 4
Hydrogen bonds in α-$BaHPO_4$; D = donor, A = acceptor.

D–H	A	*d*(D–H)/pm	*d*(H–A)/pm	Angle(DHA)/°	*d*(D–A)/pm
O11–H11	O31	99	198	166.2	295
O23–H23	O22	99	157	146.3	246
O34–H34	O33	99	149	172.7	247

4. Infrared spectroscopy

Fig. 6 shows the infrared spectrum of the title compound α-$BaHPO_4$. The IR spectra of *catena*-polyphosphates are significantly different from those of orthophosphates [19]. The characteristic bands corresponding to P–O–P vibrations in the region between 800 and 650 cm^{-1} are completely absent. The strongest bands in α-$BaHPO_4$ can be assigned to $\nu(PO^{term})$ and $\nu_{as}(PO_2)$ vibrations, respectively, and range from 1080 to 950 cm^{-1} and from 1300 to 1100 cm^{-1}, respectively. Additionally, rather intense H–O vibrations are found with a maximum at 3420 cm^{-1} typical for

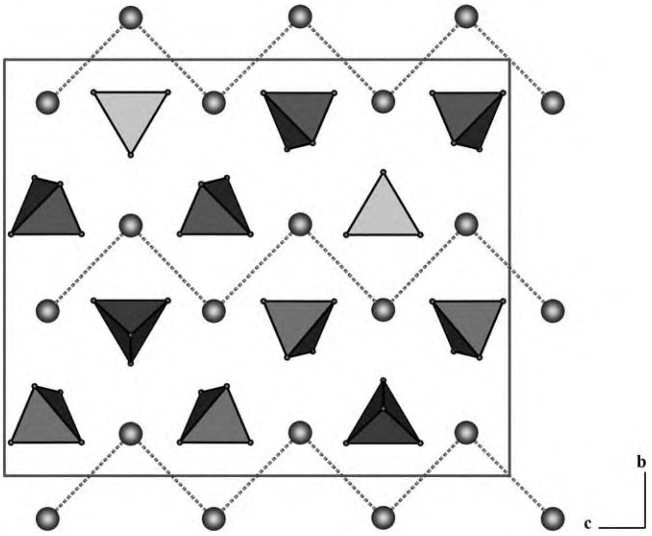

Fig. 5. Unit cell of β-$BaHPO_4$; the dotted lines clarify the sheet-like arrangement of the barium atoms.

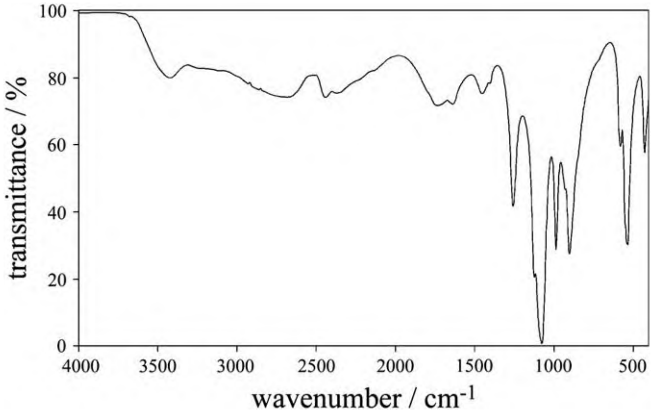

Fig. 6. Infrared spectrum of α-$BaHPO_4$.

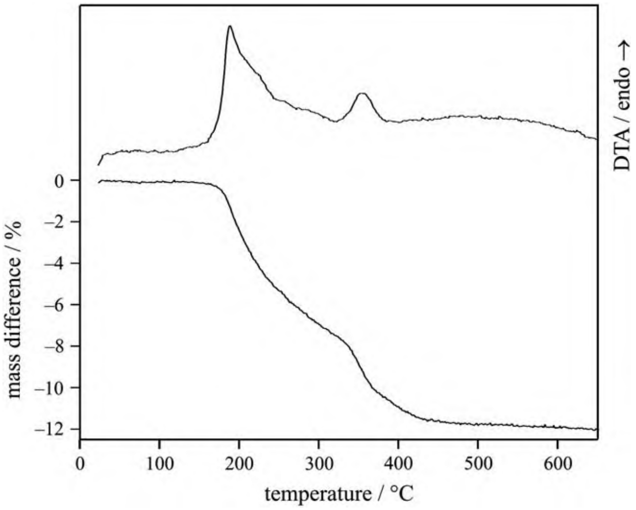

Fig. 7. Differential thermal analysis (top) and thermogravimetric diagram (bottom) of α-$BaHPO_4$.

moderately strong hydrogen bonds [17,18]. The bands found between 3000 and 1350 cm^{-1} are assigned to overtone vibrations of the strong vibrations below 1300 cm^{-1}, the band located at 2690 cm^{-1} was assigned earlier to interionic Ba–O phonon bands [6]. Thus the observed vibrational data are in good agreement with the expected values.

5. Thermal analysis

Fig. 7 shows the thermogravimetric and differential thermal analysis data of the title compound α-$BaHPO_4$. Two different endothermic caloric effects accompanied by mass losses could be detected at 191 °C (total mass difference approx. −4.5%) and 350 °C (mass difference approx. −7.5%), respectively, giving a total mass difference of 12% by heating to 650 °C. Since both effects interfere with each other it is hard to calculate the respective mass differences and therefore only approximate values are given. The initial mass loss of approx. 4.5% corresponds to the evaporation of a water molecule (theoretical mass difference: −3.9%) resulting in intermediate $Ba_2P_2O_7$ which then seems to be subject to decomposition to $Ba_3(PO_4)_2$ by loosing formal H_3PO_4 starting from α-$BaHPO_4$. Within the accuracy of the thermogravimetry this matches with the theoretical total mass difference of −14.0%. Unfortunately the reaction products are amorphous according to X-ray powder diffractometry.

Acknowledgments

The authors thank Mr. D. Saladin, Albert-Ludwigs-Universität Freiburg, for recording the infrared spectrum and Prof. Dr. H. Hillebrecht, Institut für Anorganische und Analytische Chemie, Albert-Ludwigs-Universität Freiburg, for generous support. Financial support by the Fonds der Chemischen Industrie (Liebig Habilitationsstipendium) is gratefully acknowledged.

Appendix. Supplementary material

Supplementary data associated with this article can be found, in the online version, at doi:10.1016/j.solidstatesciences.2009.05.007.

References

[1] A. Durif, Crystal Chemistry of Condensed Phosphates, Plenum Press, New York, 1995.
[2] G. Blasse, J. Alloys Compd. 192 (1993) 17.
[3] T. Jüstel, H. Nikol, C. Ronda, Angew. Chem. Int. Ed. 37 (1998) 3084.
[4] H.A. Höppe, Angew. Chem. Int. Ed. 48 (2009) 3572. doi:10.1002/anie.200804005.
[5] T. Ben Chaabane, L. Smiri, A. Bulou, Solid State Sci. 6 (2004) 197.
[6] S.K. Arora, T.R. Trivedi, A.T. Oza, V.A. Patel, Acta Mater. 49 (2001) 2103.
[7] S.K. Arora, T.R. Trivedi, V.A. Patel, Scr. Mater. 47 (2002) 643.
[8] G.M. Sheldrick, SHELXTL, V 5.10 Crystallographic System, Bruker AXS Analytical X-ray Instruments Inc., Madison, 1997.
[9] R. Hoppe, Angew. Chem. Int. Ed. 5 (1966) 95.
[10] R. Hoppe, Angew. Chem. Int. Ed. 9 (1970) 25.
[11] R. Hübenthal, MAPLE, Program for the Calculation of the Madelung Part of Lattice Energy, University of Gießen, Germany, 1993.
[12] H.A. Höppe, Z. Anorg. Allg. Chem. 631 (2005) 1272.
[13] W.H. Baur, Acta Crystallogr. B 30 (1974) 1195.
[14] T. Balic-Zunic, E. Makovicky, Acta Crystallogr. B 52 (1996) 78.
[15] E. Makovicky, T. Balic-Zunic, Acta Crystallogr. B 54 (1998) 766–773.
[16] R.D. Shannon, C.T. Prewitt, Acta Crystallogr. B 25 (1969) 925.
[17] G.A. Jeffrey, An Introduction to Hydrogen Bonding, Oxford University Press, Oxford, 1997.
[18] T. Steiner, Angew. Chem. Int. Ed. 41 (2002) 48.
[19] A. Rulmont, R. Cahay, M. Liegeois-Duyckaerts, P. Tarte, Eur. J. Solid State Inorg. Chem. 28 (1991) 207.